Neuro-Oncology
25(10), 1775–1787, 2023 | https://doi.org/10.1093/neuonc/noad076 | Advance Access date 19 April 2023

Stem-like signatures in human meningioma cells are under the control of CXCL11/CXCL12 chemokine activity

Federica Barbieri, Adriana Bajetto, Irene Dellacasagrande, Agnese Solari, Roberto Würth, Virginia Fernandez, Silvia Rancati, Davide Ceresa, Irene Appolloni, Giuseppa De Luca, Mariella Dono, Paolo Nozza, Piero Schiapparelli, Monica Gambaro, Pietro Fiaschi, Gabriele Gaggero, Nicolò Costanzo, Stefano Thellung, Paolo Malatesta, Aldo Pagano, Gianluigi Zona, Davide De Pietri Tonelli, and Tullio Florio

All author affiliations are listed at the end of the article

Present Address: Division of Stem Cells and Cancer, German Cancer Research Center, Heidelberg, Germany (R.W.)

Corresponding Authors: Tullio Florio, MD, PhD, Section of Pharmacology, Department of Internal Medicine, University of Genova, Genova, Italy (tullio.florio@unige.it); Davide De Pietri Tonelli, PhD, Neurobiology of miRNA, Istituto Italiano di Tecnologia (IIT), Genova, Italy (davide.depietri@iit.it).

Abstract

Background. Meningiomas are mainly benign brain tumors, although about 20% of histologically benign cases are clinically aggressive and recur after resection. We hypothesize that meningioma brain invasiveness and recurrence may be related to the presence of cancer stem cells and their high responsiveness to the CXCL12-CXCR4/CXCR7 chemokine axis. The aim of this study was to isolate meningioma stem cells from human samples, characterize them for biological features related to malignant behavior, and to identify the role of CXCR4/CXCR7 in these processes.

Methods. Meningioma stem cells were isolated from patient-derived primary cultures in stem cell-permissive conditions, and characterized for phenotype, self-renewal, proliferation and migration rates, vasculogenic mimicry (VM), and in vivo tumorigenesis, in comparison with differentiated meningioma cells and stem-like cells isolated from normal meninges. These cell populations were challenged with CXCL12 and CXCL11 and receptor antagonists to define the chemokine role in stem cell-related functions.

Results. Stem-like cells isolated from meningioma cultures display higher proliferation and migration rates, and VM, as compared to meningioma non-stem cells or cells isolated from normal meninges and were the only tumorigenic population in vivo. In meningioma cells, these stem-like functions were under the control of the CXCR4/CXCR7 chemokine axis.

Conclusions. We report a role for CXCL11 and CXCL12 in the control of malignant features in stem-like cells isolated from human meningioma, providing a possible basis for the aggressive clinical behavior observed in subsets of these tumors. CXCR4/CXCR7 antagonists might represent a useful approach for meningioma at high risk of recurrence and malignant progression.

Key Points

1. Meningioma contains tumor stem cells displaying signatures of aggressive phenotype.
2. Meningioma stem cells are tumorigenic in vivo after xenograft in mouse embryo brains.
3. The CXCR4-7/CXCL11-12 axis supports meningioma stem cell aggressiveness.

Importance of the Study

Recurrence in histologically benign meningiomas has been reported in several cases. Cancer stem cells are essential drivers of initiation and relapse of malignant neoplasms, whereas less is known of their role in benign lesions, including meningioma. We established cultures of patient-derived meningioma stem-like cells, characterized by a mesenchymal-like phenotype and aggressiveness hallmarks (sustained proliferation, motility, and vasculogenic mimicry), as compared to their differentiated counterpart and normal meningeal cells. Xenotransplant in embryonic mouse brains revealed that only stem-like cells successfully initiate tumors. The chemokine receptors CXCR4-CXCR7 and their ligands CXCL11-CXCL12, expressed by meningioma samples, contribute to proliferation, migration, and vasculogenic potential of meningioma stem-like cells, suggesting a functional role for these chemokines in meningioma progression. The translational implications of these findings, providing insight into meningioma biology, may serve as model to develop targeted treatments for these clinically challenging tumors, possibly focusing on CXCR4-CXCR7 chemokine axis.

Meningioma, the most frequent primary central nervous system tumor, represents ≈ 50% of all nonmalignant tumors in adults.[1] Meningiomas, classified into 3 World Health Organization (WHO) grades,[2] are mainly WHO I (≈80%) histologically benign, slow-growing neoplasms, despite morphological heterogeneity. Usually, surgery combined with fractionated radiotherapy is curative.[3] However, a subset of WHO I tumors (20%–25%) shows a negative prognosis, with unpredictable clinical course, invasive growth, and recurrence. Thus grading cannot reliably correlates with meningioma outcome, which is rather related to genotypic clusters.[4] Moreover, in these cases, the lack of effective pharmacological treatments makes almost unavoidable a bad clinical outcome.[5] To date, genetic profiling of meningiomas showing a potential correlation with aggressiveness and recurrence is not yet exploitable in clinical practice,[6] whereas information about meningioma stem-like cells and the mechanisms driving tumorigenesis and disease progression could highlight novel therapeutic options. Therefore, to identify meningioma cellular pathways responsible for malignant potential not mirrored by histologic classification, is necessary to identify novel therapeutic targets.

In malignant tumors, cancer stem cells (CSCs) are responsible for tumor initiation, invasiveness, recurrence, and drug resistance.[7,8] Putative meningioma stem cells have been reported in few studies from WHO II-III grades, on the basis of self-renewal and cluster of differentiation (CD) 133 or Sox2 expression, and tumorigenicity in mice.[9,10] Pluripotency markers Oct4 and Nanog were also identified in high-grade meningioma.[11] Notably, non-tumorigenic $CD105^+$ meningioma mesenchymal-like stem cells were isolated,[12] with the exception of $CD105^+$-cells from rhabdoid meningioma displaying high proliferation and spherogenesis rates, and the ability to differentiate into adipocytes and osteocytes and to develop tumors in mice.[13] However, these studies are limited, sometimes discordant, and analyzed cells from few, mainly high-grade tumors. Hence, at present, it is difficult to define their phenotype and biological roles.

Another relevant aspect of meningioma biology is related to cyto/chemokine release by tumor stroma or directly by meningioma cells.[14] Among these, CXCL12 and its receptors CXCR4 and CXCR7 (a.k.a. ACKR3) are key factors in inflammation and cancer. Tumor progression, angiogenesis, metastasization, and CSC maintenance depend on interactions between niche-derived CXCL12 and its receptors present on stem populations.[15] CXCL11, identified in tumor-associated vasculature, also engages CXCR7 promoting CSC self-renewal.[16] Constitutive and ligand-dependent CXCR4 homodimerization[17] or CXCR4/CXCR7 heterodimerization[18] control cancer cell chemotaxis and proliferation. CXCL12-CXCR4 axis is overexpressed in human meningiomas and modulates meningioma proliferation via autocrine/paracrine pathways,[19,20] while CXCR7 expression was associated with aggressive meningioma features.[21]

Here, we reported the presence of stem-like cells in human meningiomas, and the role of CXCR4-CXCR7 in this subpopulation. Meningioma cells were characterized for mesenchymal and stem-like profiles, proliferation rate, migration, and vasculogenic mimicry (VM). Tumor stem-like nature of these cells was further validated by in vivo transplantation in mouse embryo brains.[22] Pharmacologic blockade of CXCR4 and CXCR7 impaired CSC-related functions in stem cell population only. Our data might help to clarify the stem-like signatures regulated by CXCL11-CXCL12 axis in meningioma cells and unveil novel possible therapeutic options.

Materials and Methods

Detailed methods are available in (Supplementary Material and Methods).

Human Meningioma Samples

Seventy-two specimens were collected and de-identified from patients undergoing surgery, between 2017 and 2022 at IRCCS-Policlinico San Martino (Genova, Italy). Tumors were histologically diagnosed at Ospedale Policlinico San Martino, according to the WHO classification[2] (Supplementary Tables 1 and 2). All patients did not receive preoperative treatments. Normal meningeal specimens, were obtained from *dura mater* of patients undergoing neurosurgical procedures for pathologies other than

meningioma (Supplementary Table 3). Tissues and clinical information were obtained after written patients' informed consent, and Institutional Ethical approval by Policlinico San Martino (register#: 17/12), updated by CER Liguria (register#: 360/2019).

Primary Cell Cultures and Stem-Permissive Culture Conditions

Freshly resected meningioma tissues were dissected into 2 portions and processed for RNA isolation and cell culture.[23] Enrichment in stem-like cells was performed by selection in serum-free medium supplemented with growth factors.[24]

Patient-Derived (PD) Meningioma Xenografts

All procedures were approved by the animal welfare committee of Istituto Italiano di Tecnologia (Genova, Italy) and by the Italian Ministry of Health according to Italian D.lgs 26/2014 and European Directive 2010/63/EU. Mice were housed at IIT animal facility. Orthotopic xenotransplant in the brains of embryonic day 12.5 (E12.5) mice developing in utero was performed as described.[22]

Results

CXCL11-12/CXCR4-7 Chemokine Ligand-Receptor System is Constitutively Expressed in Human Meningiomas

CXCR4-7, and CXCL11-12 mRNAs were expressed in all 72 consecutive meningioma samples (57 WHO I, 13 II, and 2 III, Supplementary Table 1) analyzed by quantitative RT-PCR (qPCR, Supplementary Figure 1A). Patient-derived meningioma primary cultures also released CXCL12 and CXCL11, in conditioned media. CXCL12 was secreted by 11/12 primary cultures, with a mean concentration of 388.2 ± 64.2 pg/mL (range 16.2–922.5 pg/mL) (Supplementary Figure 1B), while CXCL11 secretion was detected in all the 4 analyzed cultures, with a mean concentration of 70.7 pg/ml (range 9.6-248 pg/mL) (Supplementary Figure 1C).

Isolation and Characterization of Stem-Like Cells From Human Meningiomas

To study CXCL11-12/CXCR4-7 role in meningioma stem-like cells, 50, out of the 72 specimens available, were processed, obtaining 44 (88%) patient-derived primary cultures; 6/50 (12%) were lost or contaminated (Supplementary Table 2). Remaining 22 tissue samples were not adequate (improper material collection, preservation, or quantity) for cell isolation. Meningioma cultures grew as monolayers in Matrigel™-coated plates, allowing sub-culturing in stem cell-permissive fetal bovine serum (FBS)-free medium (hereafter identified as patient-derived meningioma stem cells, PD-Mg-S). In parallel, a portion of the primary culture was maintained in 10% FBS-containing medium, representing patient-derived meningioma differentiated cells (PD-Mg-D). Both cultures were grown under the respective conditions for at least 10 days before performing experiments.

The same protocol was applied to obtain primary cultures from normal *dura mater* specimens. Two out of four tissues successfully grew either in stem cell-permissive medium (PD-NMe-S) or FBS-containing medium (PD-NMe-D).

Before selection (p0), meningioma cultures were populated by densely granulated spindle-shaped cells, although cell heterogeneity was observed (Figure 1A, a–b). At early passages (p1-p2), PD-Mg-S exhibited long processes and formed semi-confluent monolayers (Figure 1A, c–d), while tumor-matched PD-Mg-D are enlarged and flattened with marked granularity, grew vigorously during early passages, but when reached confluence often ceased proliferation (Figure 1A, e–f).

Analogously, normal meningeal cells grew out within 2 weeks from dissection to form monolayers with homogeneous morphology, characterized by flattened cells with fine branches (Figure 1A, g). PD-NMe-S were homogenously composed of elongated cells (Figure 1A, h), while PD-MNe-D appeared as flattened cells forming a dense monolayer of fibroblast-like cells (Figure 1A, i).

Differences between PD-Mg-S and PD-Mg-D were analyzed by single-cell RNA sequencing (RNA-seq) in 2 independent cultures. The selection procedure we adopted allowed a clear discrimination between stem-like and differentiated cells (Figure 1B) and, besides the expected differences between the meningiomas, a reproducible gene expression pattern was detected in both PD-Mg-S cultures, which was alternative to the pattern of PD-Mg-D cells (Supplementary Figure 2).

Due to meningioma mesenchymal origin, we explored whether mesenchymal markers are retained in primary cultures (p0) and after passaging in stem-permissive conditions (p1). Phenotyping was performed by FACS, using a panel of mesenchymal stem (CD73, CD90, CD105) and negative markers (CD14, CD19, CD31, CD34, CD45, and Human Leukocyte Antigen-DR isotype, HLA-DR).[25] Seventy-five percent of cells in p0 cultures expressed CD73, CD90, and CD105 and, even though in lower percentage, CD14, CD45, and HLA-DR, indicating monocyte/macrophage and leukocyte contamination (Figure 1C). Few $CD34^+$ and $CD31^+$ cells were also detected. In vitro selection in stem-permissive medium (p1), increased mesenchymal marker expression to more than 95% of cells, while others were drastically reduced (Figure 1C), indicating an enrichment in mesenchymal-like stem cells.

FACS immunophenotyping for mesenchymal stem marker expression in 6 PD-Mg-S and PD-Mg-D and normal meninges cultures (Figure 1D and Supplementary Figure 3), showed no difference in CD73, CD90, and CD105 levels, although the percentage of positive cells varied among groups. CD90 and CD105 expression, analyzed by western blotting in 4 tumor-matched stem-like and differentiated cells, confirmed the lack of specificity of their expression in the stem cell subpopulation (Figure 1E, quantified in Supplementary Figure 4).

Meningioma cell stemness, was tested evaluating mesenchymal multipotency. Osteogenic differentiation occurred in 3/6 PD-Mg-S cultures and in 2/2 PD-NMe-S analyzed (Figure 1F, Supplementary Figure 5). Adipogenic

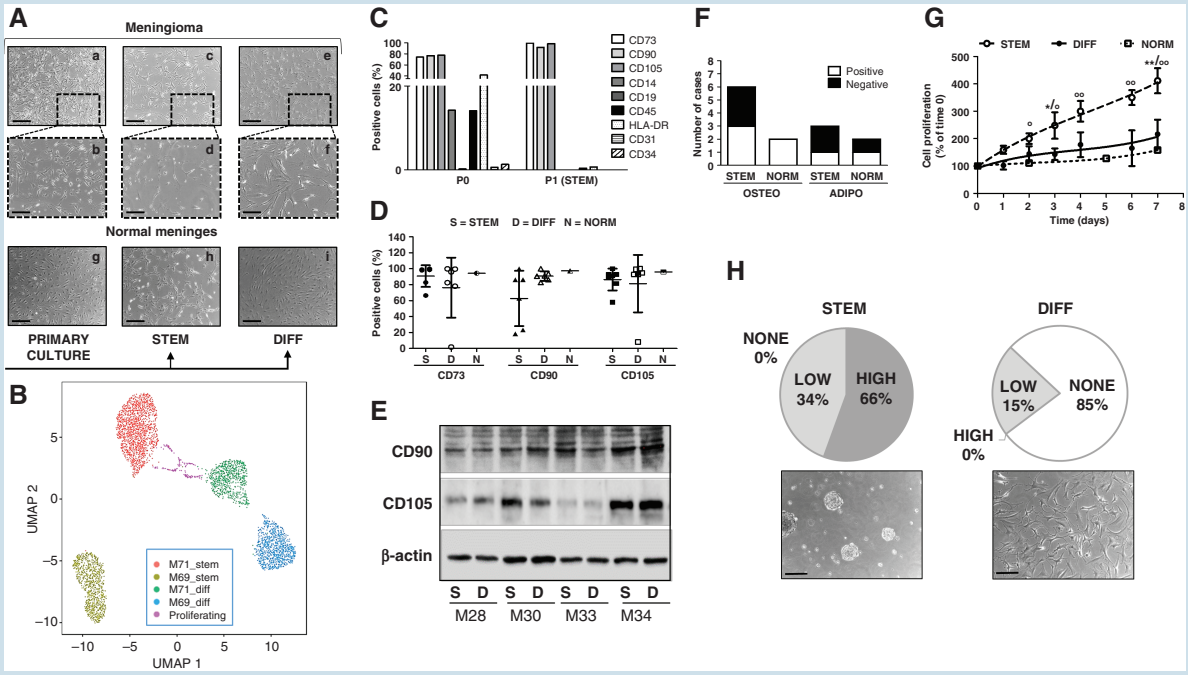

Figure 1. Isolation and characterization of patient-derived stem-like and differentiated cells from meningiomas. (A) Representative images of meningioma primary culture morphology (**a-b-g**) after selection in stem-permissive medium (STEM, **c-d-h**) or maintained in serum-containing medium (DIFF, **e-f-i**). Scale bars: 150 μm (**a-c-e-g-h-i**), 50 μm (**b-d-f**). (B)Uniform Manifold Approximation and Projection representation of single cell RNA-seq profiles of PD-Mg-S (stem) and PD-Mg-D (diff) isolated from M69 and M71. Dots are colorized accordingly the PCA clustering of their profile. A small number (about 1.2%) of monocytes and CD8 T lymphocytes were also detected, representing residual cells persisting since few passages from the primary culture were performed (not reported in the graph for sake of clarity). (C) Flow-cytometry analysis of mesenchymal markers (CD73, CD90, and CD105) and negative indicators (CD14, CD19, CD31, CD34, CD45, and HLA-DR). p0 cultures display a mesenchymal stem cell profile in a mixed population, while p1, grown in the STEM medium (PD-Mg-S), showed homogeneous $CD73^+/CD90^+/CD105^+$ phenotype and depletion of hematopoietic and endothelial contaminants. (D) Flow-cytometry analysis comparing $CD73^+/CD90^+/CD105^+$ in PD-Mg-S (STEM), PD-Mg-D (DIFF) ($N = 6$) and PD-NMe-S (NORM), at p2. Scatter dot plots depict percentage of marker positive cells from individual cultures; lines represent mean ± SD. (E) Representative immunoblots of CD90 and CD105 expression in PD-Mg-S and PD-Mg-D matching cultures ($N = 4$, tumor ID#: M28-M30-M33-M34). β-actin was used as reference for protein loading. Densitometric analysis is reported in Supplementary Figure 4. (F) Stacked bar chart shows the number of cultures able to differentiate into osteogenic and adipogenic lineages (white) on the total of PD-Mg-S ($N = 6$) and PD-NMe-S ($N = 2$) examined. (G) Growth curves of cultures demonstrating the sustained proliferation of PD-Mg-S as compared to matched PD-Mg-D ($N = 6$), and PD-NMe-S ($N = 1$). Each point represents mean ± SD of the cumulative time-course expressed as percentage of respective time 0. (H) Analysis of sphere-formation from low density meningioma cultures. Pie charts show that all PD-Mg-S ($N = 9$) generate meningospheres with high or low efficiency, while only 15% sphere-forming cultures originated from the corresponding PD-Mg-D. Phase-contrast images of 10 days–cultures depict representative tumor spheroids in stem (scale bar: 100 μm) and differentiating (scale bar: 50 μm) conditions.

differentiation was carried out in 3 PD-Mg-S and 2 PD-NMe-S, it was detected in only one culture from each group (Figure 1F).

Then we characterized meningioma cell proliferation in time-course experiments by CyQuant™ assay: PD-Mg-S ($n = 6$) grew faster than PD-Mg-D, isolated from the same tumor, or PD-NMe-S, with a mean doubling time of 3.3 days versus 6.5 and 11.3 days, respectively (Figure 1G). Stem cell-permissive conditions allowed a constant proliferation for up to 7 days in most cultures, while PD-Mg-D growth arrests within 2–3 days. Notably, each of the 6 cultures evidenced a different growth profile, denoting individual, and heterogeneous proliferative activity (Supplementary Figure 6). The assessment of mutational burden of 16 meningiomas, from which we isolated stem-like cells, evidenced the presence of pathogenic mutation of SMO, AKT1, KLF4, pTERT, and KIT1 in 50% of the tumors (Supplementary Table 4). However, we did not find correlations between the presence of mutations and the proliferation rate. We observed, only in one PD-Mg-D culture (M34) bearing AKT1 mutation, a proliferation rate much higher than all the other PD-Mg-D cultures (Supplementary Figure 7).

Self-renewal potential was evaluated by sphere-formation assay in 11 PD-Mg-S and the differentiated counterparts, upon 7-day culture in serum-free medium without Matrigel™. Emergence of floating meningospheres with low (34%) or high (66%) efficiency (as for number and size) was observed in all PD-Mg-S, while PD-Mg-D, grown in stem conditions, gave rise to small aggregates (15%) or remained adherent (no spheres formed, 85%) (Figure 1H), confirming that PD-Mg-S are enriched in cells with stem-like features. By extreme limiting dilution analysis performed on two meningiomas,

we identified self-renewal ability in about 1/2985 (M69) and 1/5624 cells (M71)(Supplementary Figure 8). No sphere-forming ability was detected in the PD-Mg-D from the same meningiomas.

Meningioma Stem-Like Cells Exhibit a Prevalent Mesenchymal Phenotype

Meningioma cell phenotype was analyzed by immunofluorescence (IF), comparing eight matched PD-Mg-S and PD-Mg-D and 2 PD-NMe-S cultures (Figure 2A, B). Epithelial membrane antigen (EMA), a typical meningioma marker, was expressed mainly in PD-Mg-D and PD-NMe-S, but only in 50% of PD-Mg-S. PD-Mg-S mesenchymal profile was further confirmed, in all cultures tested, by CD44 expression, a cell-adhesion molecule related to cancer invasion and stemness, and vimentin, a type III intermediate filament. N-cadherin, involved in epithelial-to-mesenchymal transition (EMT) and tumor aggressiveness, was detected in all PD-Mg-S (7/7), while 2/5 expressed E-cadherin. N-cadherin$^+$ and E-cadherin$^+$ cells were detected in 2/7 and 3/5 PD-Mg-D cultures, respectively (Figure 2B). Similar immunoreactivity pattern was observed in PD-NMe-S. All meningioma cells and PD-NMe-S, independently from the culture conditions, showed a diffuse staining for the stem marker nestin, while CD133 was more expressed in PD-Mg-S (3/4), although appearing in scattered PD-Mg-D cells (Figure 2A, B). Similarly, by qPCR, we found comparable SSTR2 expression in both PD-Mg-s and PD-Mg-D cells isolated from 6 meningiomas (Figure 2C, D). Sox2 and Oct4 levels, assessed by western blotting (Figure 2E, F), did not differ between PD-Mg-S and PD-Mg-D. These data were also corroborated by single-cell RNA-seq we performed in two pairs of PD-Mg-S and PD-Mg-D, showing enrichment in genes encoding for EMT and reduction of cell-to-cell adhesion in PD-Mg-S (Supplementary Figure 9), while no significant differences in stem-like markers were observed (data not shown), Overall, although we did not find marked differences, PD-Mg-S cells displayed a more defined mesenchymal phenotype, with PD-Mg-D cells showing more epithelial-like characteristics.

Meningioma Stem-Like Cells Have Distinctive Functional Features Sustaining an Aggressive Phenotype and Tumorigenicity In Vivo

Given the predominant mesenchymal-like phenotype of PD-Mg-S, we investigated, in a transwell assay, the chemotaxis of fluorescently-labeled cells toward 10% FBS. Migratory activity was significantly higher in PD-Mg-S ($n = 11$) as compared to PD-Mg-D ($n = 8$) (Figure 3A,

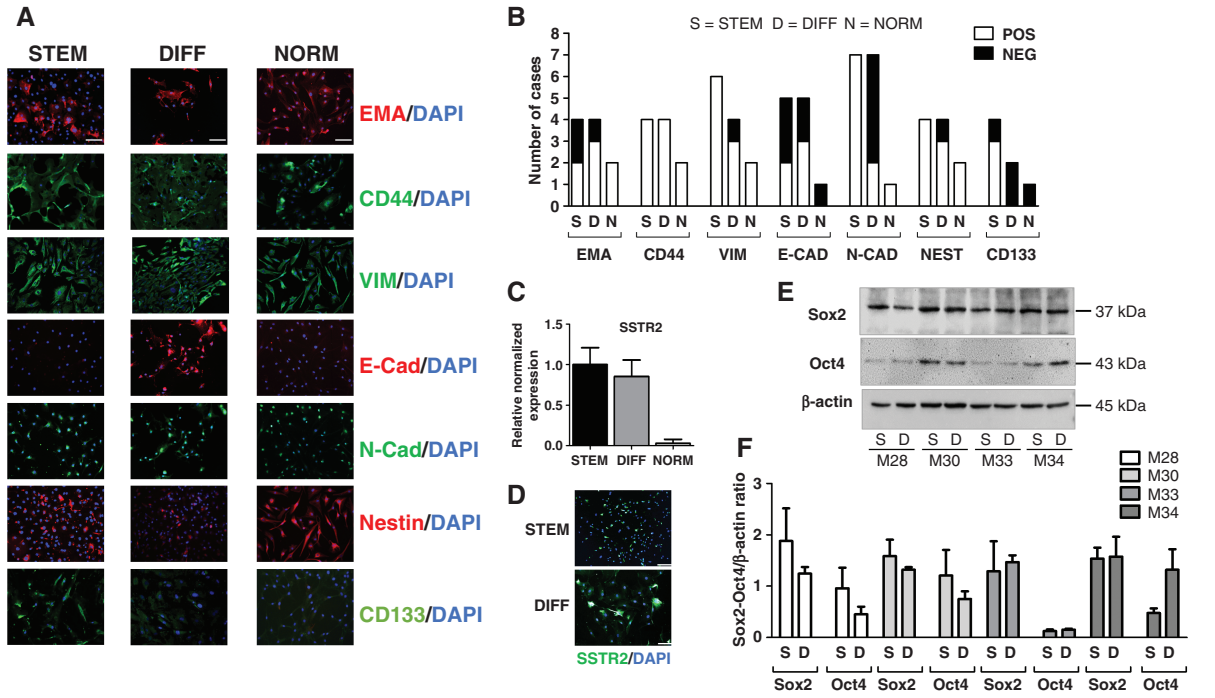

Figure 2. Pattern of expression of markers in meningioma stem-like cells and differentiated counterpart. (A) Representative IF images of PD-Mg-S, PD-Mg-D, and PD-NMe-S showing markers' expression within cell monolayers. Scale bars: 100 μm. (B) Stacked bar graph depicting the IF results of Figure 2A, as the number of positive (white) and negative (black) cultures. (C) Quantitative RT-PCR analysis of SSTR2 mRNA levels in PD-MG-S and PD-Mg-D cultures (N = 6). Histogram shows the mean ± SD of tested cultures. (D) SSTR2 expression in PD-Mg-S and PD-Mg-D cells. Representative IF images are reported. Scale bars: 100 μm. (E) Representative immunoblots for Sox2 and Oct4 in PD-Mg-S and PD-Mg-D matching cultures ($N = 4$, tumor ID# M28-M30-M33-M343). β-actin was used as reference for protein loading. (F) Histogram reports the densitometric analysis of normalized protein levels.

Supplementary Figure 10A shows the direct comparison between PD-Mg-S and PD-Mg-D from the same tumor).

Considering the high vascularity of meningiomas and the ability of CSCs to imitate endothelial cells through VM,[26] we evaluated the propensity of PD-Mg-S ($n = 7$) to promote vessel-like assembly in vascular-endothelial growth factor (VEGF)-containing medium. The proangiogenic response after o/n VEGF stimulation, quantified by branch and loop counting within the formed tubes, was significantly higher in PD-Mg-S than in PD-Mg-D (Figure 3B, Supplementary Figure 10B shows the direct comparison between PD-Mg-S and PD-Mg-D from the same tumor). Higher VEGF responsiveness is supported by a higher expression of VEGFR2 mRNA in PD-Mg-S compared to PD-Mg-D counterpart (≈12-fold, Supplementary Figure 11A). Endothelial transdifferentiation ability of PD-Mg-S was further confirmed by qPCR analysis after 24 and 72 hours of incubation in VEGF-containing medium, causing a significant increase in mRNAs for the endothelial markers CD31 and CD34, vascular-endothelial cadherin and VEGFR2 itself, but not for α-smooth muscle actin (Supplementary Figure 11B, C).

In vivo, tumor-initiating ability is the main defining feature of CSCs. We evaluated the propensity to generate patient-derived xenografts (PDX) by orthotopic injection of dsRed-(DiI)-labeled PD-Mg-S in the lateral ventricle of E12.5 mouse embryos (Figure 3C, a–b). Analysis at E18.5 or postnatal day 0 showed that embryonic brains support the growth of PD-Mg-S (Figure 3C ,c-d; success rate for xenograft generation: 30%, Supplementary Table 5). IF analysis for the human-specific nuclear antigen (HuNu) confirmed the human origin of engrafted cells, and EMA expression was similar to parental human meningiomas (Figure 3C, e–f). Importantly, only PD-Mg-S gave origin to tumors, while neither PD-Mg-D nor PD-NMe-S transplants produced tumor masses (Supplementary Table 5), and only scattered cells were detected in the meninges or spread within brain parenchyma (Figure 3D, Supplementary Figure 12A, B). PD-Mg-S-derived tumors showed Ki-67$^+$

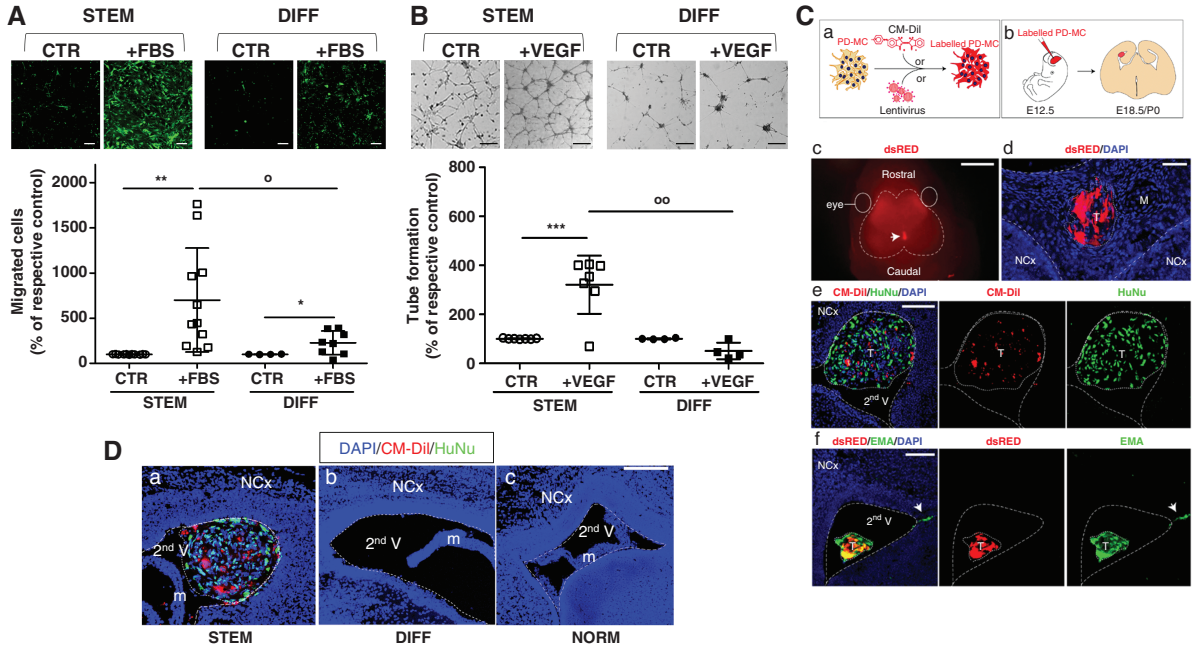

Figure 3. Meningioma stem-like cells show migratory and vasculogenic potential in vitro and tumorigenesis in vivo. (A) Representative photomicrographs of transwell migration assays of green fluorescent-labeled PD-Mg-S ($N = 11$) and PD-Mg-D ($N = 8$). Scatter dot plot depicts the quantification of transmigrated cells toward FBS in each culture. Migration was assessed after 16 hours to avoid interference of cell proliferation. Lines represent mean ± SD $^*P < .05$, $^{**}P < .01$ versus respective control (CTR); $^\circ P < .05$ versus FBS chemoattractant. Scale bar: 200 μm. (B) Representative photomicrographs of tube formation in the presence of VEGF. Capillary-like networks were more efficiently formed by PD-Mg-S ($N = 6$) as compared to PD-Mg-D ($N = 4$). Scatter dot plot shows the statistical results of the quantification of each culture. Lines represent mean ± SD. $^{***}P < .001$ versus respective control (CTR); $^{\circ\circ}P < .01$ versus VEGF stimulation. Scale bar: 50 μm. (C)WT embryonic mouse brain supports PD-Mg-S growth. **a)** Method for cell labeling using CM-DiI or lentivirus-expressing dsRED or GFP. **b)** Cell were transplantated within second ventricle (V) of E12.5 embryos, brains were analyzed post-transplantation at E18.5-P0. **c)** Dorsal view of a mouse head at E18.5; arrow: dsRED$^+$ xenograft; dashed lines: Brain boundaries. **d)** IF image of PD-Mg-S mass in the mice meninges, coronal cryosections through embryonic brains; red: dsRED$^+$ tumor (T) cells; dashed lines: Meninge (M) boundaries; NCx: Neocortex. **e)** IF images of PD-Mg-S in the secondV of embryonic brains; red: CM-DiI$^+$PD-Mg-S; green: HuNu$^+$; dashed lines: V boundary; dotted line: T mass. **f)** images of PD-MC in the secondV of embryonic brains; red: dsRED$^+$ PD-Mg-S; green: Epithelial membrane antigen (EMA). Dashed lines: V boundary; dotted line: T mass; arrow: EMA$^+$ cells invading the host parenchyma. Nuclei are counterstained with DAPI (blue). Scale bars: c) 2 mm; d) 100 μm; e) and f) 200 μm. (D) Patient-derived xenografts (PDX) are only detected upon transplantation of PD-Mg-S in WT embryonic mouse brain. IF image of cells in mice secondV analyzed at E18.5-P0. Blue: Nuclei (DAPI), red: CM-DiI$^+$ PD-Mg-S (STEM) and PD-Mg-D (DIFF), or GFP$^+$ PD-NMe-S (NORM); dashed lines: V boundary; dotted line: tumor (T). Neocortex (NCx); mouse meninges (m). Scale bar: 200 μm.

proliferating cells, and phospho-histone H3+ late G2 and mitotic cells (Supplementary Figure 13), indicating that tumor masses are actively growing. PD-Mg-S cells are also characterized by radioresistance, showing no (M69) or limited (M71) cytotoxicity when exposed up to 20 Gy (Supplementary Figure 14).

Meningioma Stem-Like Cells Express Chemokines and Chemokine Receptors

CXCL12-CXCR4 and CXCL11/12-CXCR7 pathways are upregulated in several tumor CSCs,[15] including meningioma. We did not observe changes in the expression of this chemokine axis according to meningioma grade. This observation was corroborated by the analysis of available datasets (RNA-seq Illumina: GSE183653, $n = 185$ and GSE189672 $n = 110$; microarray Affymetrix GSE16581 $n = 68$), which confirmed the absence of a clear correlation between CXCL12-CXCR4 and CXCL11/12-CXCR7 expression and meningioma grade, Ki-67 (MIB-1) index, recurrences, or the presence of necrosis (Supplementary Figure 15). We detected, only within the GSE189672 dataset, a modest relationship between CXCL11 expression and meningioma grade I ($P < .05$) and lower MIB-1 index (r2 –0,37), while CXCR4 expression correlates with grade II tumors ($P = .05$) and showed a trend toward higher expression in relapsing meningioma ($P = .07$). However, it should be noted that these datasets reflect the global expression levels in the tumors and are not ideal to address gene expression in subpopulations as meningioma stem-like cells. Thus, we analyzed the actual expression and functional role of this chemokinergic network in PD-Mg-S. qPCR results revealed that CXCR4 and CXCL11 are upregulated in these cultures, while corresponding PD-Mg-D overexpressed CXCR7 and CXCL12 (Figures 4A, B), although comparable protein levels were detectable by IF in both PD-Mg-S, PD-Mg-D, and PD-MeN-S (Figure 4C, Supplementary Figure 16).

CXCR4 and CXCR7 activation by CXCL11 and CXCL12, led to phosphorylation of ERK1/2 MAP kinase pathway in both PD-Mg-S and PDS-MG-D cells, but only in PD-MG-S cells CXCL12 was able to elicit an increase in intracellular [Ca^{2+}] (Supplementary Figure 17 and 18), indicating a different signaling ability of the receptors in these cell populations.

In vivo, PD-Mg-S-derived tumors express both CXCR4 and CXCR7, underlying the correspondence of this PDX model with parental tumors. CXCR7 and E-cadherin expression, which in vitro mainly characterizes PD-Mg-D, in PD-Mg-S xenografts indicates that, as expected for CSC-derived tumors, a differentiation process occurs within tumor mass once implanted in receptive tissues (Figure 4D).

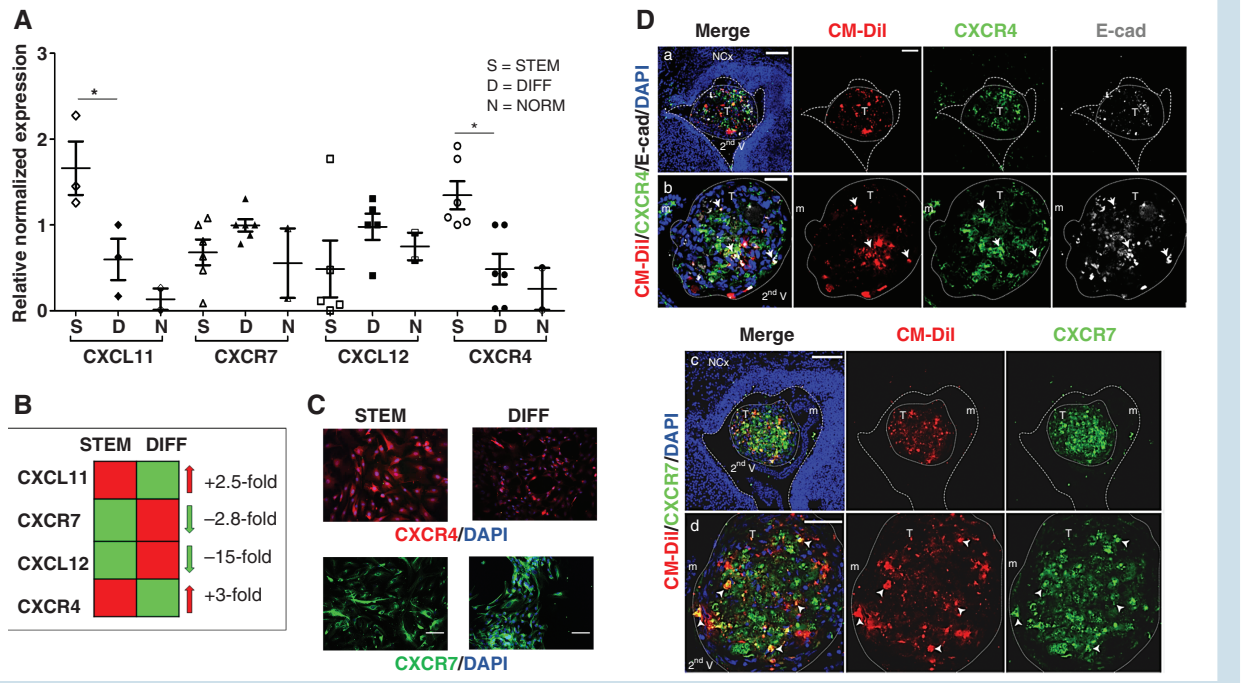

Figure 4. Differential expression of CXCR4 and CXCR7 and their ligands in meningioma-derived cultures and xenografts. (A) Chemokine ligands and receptors mRNA levels in PD-Mg-S and PD-Mg-D ($N = 6$) and PD-NMe-S ($N = 2$). Scatter dot plot reports individual cultures. Lines represent mean ± SD. *$P < .05$. (B) Fold changes of gene expression for CXCR4 and CXCL11 and CXCR7 and CXCL12 in PD-Mg-S in comparison to PD-Mg-D. (C) Representative IF images showing CXCR4 homogenously expressed in PD-Mg-S cells and CXCR7 is restricted to cell subsets. Blue: Nuclei (DAPI). Scale bars: 100 μm. (D) Xenotransplants of PD-Mg-S express CXCR4 and CXCR7. IF image of cells transplanted in the mouse embryo second V analyzed at E18.5-P0. **a, b**) Cells expressing CXCR4 (arrow). Note the expression of CXCR4 in host murine meninges (m). **c, d**) Cells expressing CXCR7 (arrowheads). Blue: nuclei (DAPI); red: CM-DiI+; green: CXCR4; gray: E-Cadherin (**a, b**); green: CXCR7 (**c, d**). Dashed lines: tissue boundary; dotted line: tumor (T) boundary. NCx: Neocortex. Scale bars: a, c) 100 μm; b) 35 μm; d) 50 μm.

CXCL11 and CXCL12 are Main Regulators of Relevant Biological Activities in Meningioma Stem-Like Cells

To assess CXCR4/CXCR7 role in cell proliferation, growth factor- or FBS-starved PD-Mg-S, PD-Mg-D, and PD-NMe-S cultures were treated with CXCL11 and CXCL12. Both chemokines significantly enhanced PD-Mg-S proliferation (+52% and + 38% vs. controls, respectively, see Supplementary Figure 19 for the direct comparison of PD-Mg-S and PD-Mg-D from the same tumor), whereas PD-Mg-D and PD-NMe-S were unaffected (Figure 5A). Moreover, CXCL11 and CXCL12, used as chemoattractants, significantly enhanced basal PD-Mg-S migration (+41% and + 33%, respectively), while no effect was observed in PD-Mg-D (Figure 5B). Finally, PD-Mg-S exhibited a significantly higher ability to form tubular structures after exposure to CXCL11 (+46%) and CXCL12 (+89%) than PD-Mg-D (Figure 5C). The increased propensity of PD-Mg-S cells to undergo VM was also confirmed in vivo by the identification of CD31-immunoreactivity in tumor masses developed after xenotransplant in the embryonic model. In order to address whether PDX from transplanted PD-Mg-S cells could develop new vessels, we analyzed 2 representative tumors: one developed in the brain parenchyma in proximity of the meninges (Figure 5D a,b,c,d) and a second one grown inside the ventricle (Figure 5D e,f,g,h,i). In the latter case, considering the distance of the tumor mass from the host brain parenchyma, we postulated that the CD31$^+$ cells are likely deriving from PD-Mg-S themselves.

Therefore, independently from the relative CXCR4 and CXCR7 expression, PD-Mg-S display higher sensitivity to chemokine-dependent proliferation, migration, and VM than PD-Mg-D. Mechanistically, these distinct responses may be related to the different intracellular signaling activated in these cell populations by CXCL12 (see Supplementary Figures 17 and 18). In the available cases,

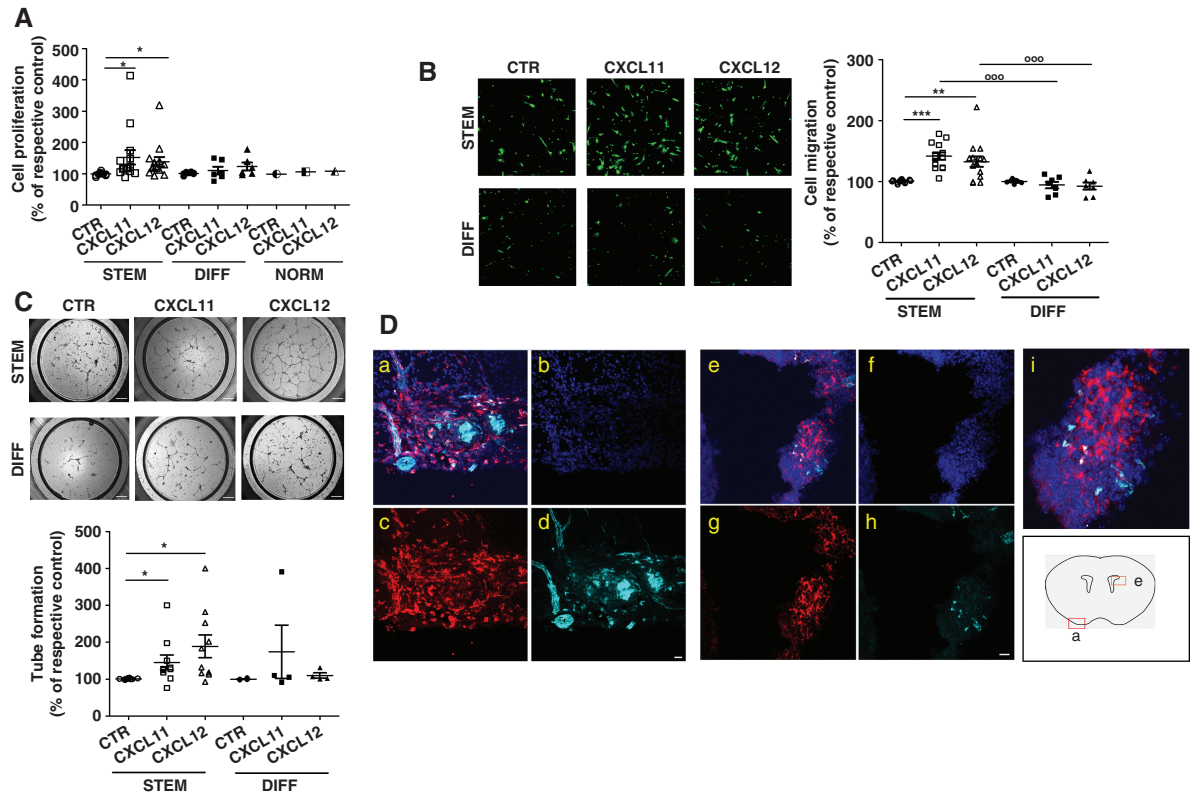

Figure 5. CXCL11-12/CXCR4-7 system supports proliferation, migration, and neo-angiogenesis in meningioma stem-like cells. (A) In vitro proliferation of PD-Mg-S ($N = 11$), PD-Mg-D ($N = 6$), and PD-NMe-S treated with CXCL12 or CXCL11 for 24 hours. Scatter dot plot depicts the percentage of cell proliferation versus vehicle-treated controls (CTR, 100%); lines represent mean ± SD. Each point represents one individual tumor. *$P < .05$ versus respective CTR. (B) Representative photomicrographs of transwell migration of green-fluorescent PD-Mg-S ($N = 14$) and PD-Mg-D ($N = 7$) toward CXCL11 or CXCL12 (25 nM). Scale bar: 200 μm. Scatter dot plot depicts the quantification of transmigrated cells in each culture. Each points represents one individual tumor. Lines represent mean ± SD. **$P < .01$ and ***$P < .001$, versus respective control (CTR, 100%), °°°$P < .001$ versus chemokine stimulation. Scale bar: 150 μm. (C) Representative photomicrographs of tube networks formed by PD-Mg-S ($N = 10$) or PD-Mg-D ($N = 4$), after exposure to CXCL11 or CXCL12 (25 nM). Scatter dot plot shows the quantification of tube formation. Each points represents one individual tumor. Lines represent mean ± SD. *$P < .05$ versus respective control (CTR, 100%). (D) PD-Mg-S-derived PDX in mouse embryo contain CD31$^+$ cells. Images depict two independent tumors: Panels a-d refer to a mass developed in the host brain parenchyma in proximity of the meninges; panels e-h depict a tumor mass developed inside the second ventricle. Panel i is an enlargement of panel e. Injected PD-Mg-S were stained with Ds Red (red), nuclei counterstained with Hoechst (blue), and CD31 staining is evidenced in cyan (Alexa Fluor®647). Scale bar: 20 μm.

we did not find correlations between mutational status and chemokine responses (Supplementary Figure 20).

To assess the individual contribution of CXCR4 and CXCR7 in CXCL12- and CXCL11-mediated signaling, we treated PD-Mg-S with AMD3100 and CCX771, antagonists of CXCR4 and CXCR7, respectively.[27,28] Both antagonists did not affect PD-Mg-S basal proliferation, migration, and tube formation as well as ERK1/2 activation but caused a significant reduction of these functions induced by CXCL11 and CXCL12 (Figure 6A,B). Finally, we used 3D cultures[29,30] of PD-Mg-S and PD-Mg-D cells to assess CXCR4 and CXCR7 role in tumor development. We confirmed in vivo studies (see Figure 3D) showing that differentiated cells are unable to develop 3D cultures, as for their non-tumorigenic nature. However, in the presence of AMD3100 and/or CCX771, PD-MG-S cells were still able to grow as 3D structures, suggesting that these receptors are not involved in tumorigenesis but rather in tumor progression and spreading (Supplementary Figure 21).

Thus, CXCL11 and CXCL12 sustain the aggressive phenotype of PD-Mg-S and, possibly, progression and diffusion of meningiomas. Since individual blockade of each of chemokine receptors completely abolished CXCL11 (CXCR7 agonist) and CXCL12 activity (CXCR4/CXCR7 agonist), the effects of these chemokines are likely mediated by the formation/activation of CXCR4-CXCR7 heterodimers (Figure 6C).

Discussion

Different meningioma classifications based on genetic analyses were proposed to obtain a more reliable prognostic evaluation as compared to the classical histological grading.[4,31] However, besides genetic components, tumor cell subtypes, and, in particular, tumor stem cells, populating the tumor mass may also contribute to the tumor clinical behavior. We report the successful isolation and culture enrichment of stem-like cells from a large cohort of meningioma specimens, reflecting clinical (age, sex, and localization) and histopathological (grade, subtype) features commonly observed in meningioma patients.[1] Primary cultures from the same meningioma, cultured in differentiation medium, allowed us to grow non-stem/differentiated cell counterpart, modeling the cells composing the meningioma mass. Single-cell RNA-seq of both PD-Mg-S and PD-Mg-D validated this selection approach, revealing that the 2 populations are clearly distinct, without cross-contamination within a single meningioma, and that PD-Mg-S cells from independent tumors (as well as PD-Mg-D cells) display a common transcriptomic signature.

Thus meningiomas contain stem-like populations likely involved in tumor progression, as shown in other benign tumors such as pituitary adenomas[32] and schwannomas.[33] Furthermore, the reported presence of embryonic stem cell markers in grade I meningiomas, indirectly supports our observation.[34]

The comparison of tumor-relevant in vitro biological properties in different cell subsets from the same tumor, was instrumental to define PD-Mg-S specific features. PD-Mg-S characterization demonstrated that they are the only meningioma population endowed with CSC features: sustained in vitro proliferation, self-renewal, growth as 3D structures, and in vivo tumorigenic ability. Data on meningioma CSCs are scanty and controversial, likely due to the small and heterogeneous series of tumors previously analyzed. CD105$^+$ tumor-initiating cells were described in one rhabdoid meningioma,[13] and in meningioma cultures xenotransplanted in NOD/SCID mice,[35,36] while injection of different mesenchymal meningioma stem-like cells did not originate tumors.[12] Here, we assayed human meningioma cell tumorigenicity by orthotopic engraftment of PD-Mg-S in the embryonic mouse brains, a model which allows the development of tumors after only few days from xenotransplantation.[22] We demonstrate engraftment and proliferation of EMA-expressing PD-Mg-S, while neither PD-Mg-D nor normal meningeal cells generate tumors. PD-Mg-S-tumors express E-cadherin in vivo, which replaced N-cadherin expressed in vitro when cultured in stemness-supporting conditions, indicating a switch toward a differentiated phenotype, likely supported by the brain microenvironment.

Several markers have been proposed to identify CSCs, although specific phenotypes have not been identified. High-grade meningiomas express CD133[37] sometimes altogether with CD44, nestin, Sox2, or vimentin.[38,39]

However, no studies explored the differential phenotype between CSCs, non-stem tumor cells, and normal meningeal cells, as here reported. Unexpectedly, none of these markers represents an exclusive PD-Mg-S signature. Neither pluripotency transcription factors (Oct4, Sox2), stem markers (ie, nestin), nor SSTR2, a prognostic meningioma marker,[40] were differentially expressed among PD-Mg-S, PD-Mg-D, and PD-NMe-S. Only CD133, marker of progenitor/stem cells,[36–39] was actually detected in most PD-Mg-S cultures but not in PD-Mg-D or PD-NMe-S. In addition, most cultures expressed EMA and vimentin, reflecting the dual epithelial/mesenchymal nature observed during meningeal development, and suggesting that the origin of stem-like cells might be unrelated to the cognate adult tissue.[41]

The most striking phenotypical difference between PD-Mg-S and PD-Mg-D is N-cadherin expression, which was specific for the stem-like cultures, supporting altogether with vimentin expression, their mesenchymal phenotype. Moreover, PD-Mg-S cells show reduced E-cadherin, which is consistent with high motility and invasiveness we report, and also observed in recurrent WHO grade I tumors,[42] likely favoring the relapse of histologically benign meningiomas.[43] This observation was confirmed by single-cell RNA-seq experiments showing a higher expression of EMT-related genes in PD-Mg-S, and of genes related to epithelial cell-to-cell adhesion in PD-Mg-D, further supporting the possible role of PD-Mg-S subpopulation in meningioma cells spreading and tumor relapse.

CD73[44]- and CD105[13]-expressing non-tumorigenic mesenchymal-like meningioma stem cells can differentiate into osteocytes, adipocytes, and chondrocytes. However, in these studies, cultures were obtained from only 2/10 WHO grade II meningiomas, and CD105$^+$ cells populated tumor microenvironment (TME) rather than the tumor mass.[12] In our study, both PD-Mg-S and PD-Mg-D express

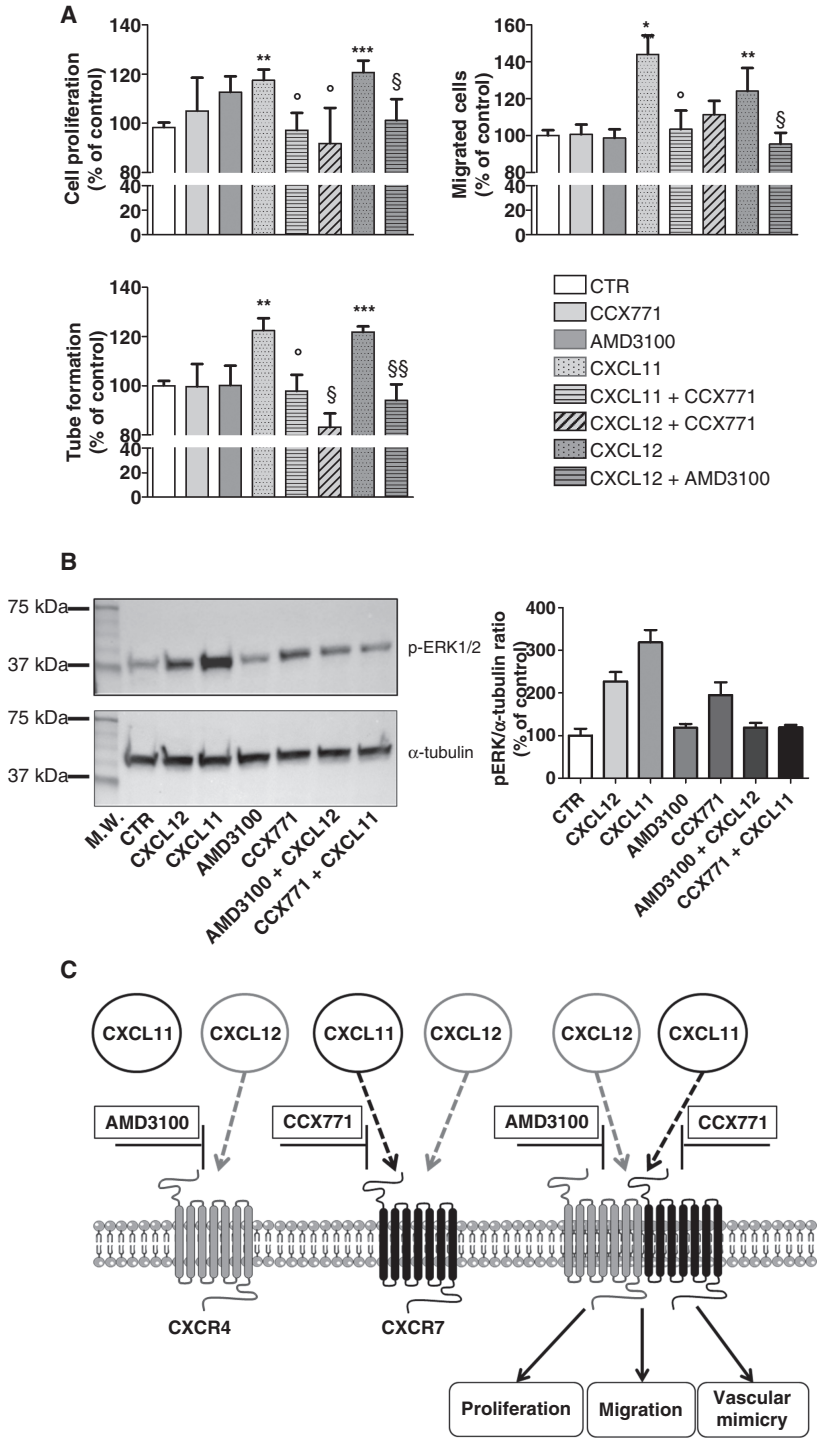

Figure 6. Pharmacologic inhibition of CXCL11 and CXCL12 impairs meningioma stem-like cell activity. (A) (Upper left panel) Antiproliferative effects of CXCR4 (AMD3100) and CXCR7 (CCX771) inhibitors in PD-Mg-S ($N = 7$) stimulated with CXCL11 or CXCL12 (25 nM). Bars represent mean ± SD of the percentage of vehicle-treated controls (CTR). $^{**}P < .01$ and $^{***}P < .001$ versus respective CTR; $^{\circ}P < .05$ *versus* CXCL11; $^{\S}P < .05$ versus CXCL12. (Upper right panel) Migrastatic effects of AMD3100 and CCX771 in CXCL11 or CXCL12 (25nM) -stimulated PD-Mg-S ($N = 3$). $^{*}P < .05$ and $^{**}P < .01$ versus respective CTR; $^{\circ}P < .05$ versus CXCL11; $^{\S}P < .05$ versus CXCL12. (Lower left panel) Inhibition of CXCL11- and CXCL12-mediated vessel-like formation by AMD3100 or CCX771 in PD-Mg-S ($N = 2$). $^{**}P < .01$ and $^{***}P < .001$ versus respective CTR; $^{\circ}P < .05$ versus CXCL11; $^{\S}P < .05$ and $^{\S\S}P < .01$ versus CXCL12. (B) Inhibition of ERK1/2 activation induced by CXCL12 and CXCL11 by treatment with AMD3100 and CCX771. Left panel: Representative WB using phospho-ERK1/2 (upper panel) and α-tubulin (lower panel). Right panel: Densitometric analysis showing the pERK1/2-α/tubulin ratio. (C) Schematic diagram showing the ability of CXCR4 and CXCR7 antagonists (AMD3100 and CCX771), individually added, to completely prevent meningioma stem-like cell proliferation, migration and tube formation, induced by both CXCL11 and CXCL12.

mesenchymal markers, thus neither CD105 nor other mesenchymal antigens (CD73, CD90) univocally define the stem-like subpopulation. Conversely, a mesenchymal-like phenotype (markers and osteogenic differentiation ability) is conserved in both stem and differentiated cells, implying that multipotent mesenchymal cells, driving embryonic meningeal development, are relevant for meningioma genesis.[41] Further studies are needed to address this issue, nevertheless, since meningiomas cells have been reported to co-express mesenchymal markers,[9,12,13,44] our data corroborate the hypothesis that the mesenchymal phenotype is predominant in meningioma stem cells.

To overcome phenotypical uncertainty, functional validation is crucial for *bona fide* meningioma stem cell identification. PD-Mg-S cells display higher proliferative rate, self-renewing ability, and migratory and VM activities compared to PD-Mg-D, possibly reflecting a clinically aggressive behavior. Invasiveness of anaplastic meningioma stem-like cells correlated with KLF4 downregulation[10] and miRNA-145 expression in atypical and anaplastic meningiomas,[45] while no data are to date available for benign lesions. Here, we demonstrate that cells endowed with stem-like features are detectable in grade I meningiomas, likely becoming predominant when an unpredictable aggressive behavior occurs.

CSC's impact on cancer growth, invasiveness, and neoangiogenesis is not only dependent on cell distinctive properties but also through interaction with TME. CXCL12-CXCR4 axis, allowing CSC-TME crosstalk, is a main regulator of CSC biology promoting cancer initiation and progression.[46,47] Starting from the reported role of the CXCL11-12/CXCR4-7 system in meningioma,[19–21] we show that both receptors and ligands are expressed in most meningiomas, and that CXCL12 and CXCL11 are secreted by primary cultures. In PD-Mg-S, CXCR4 and CXCL11 are preferentially expressed, while PD-Mg-D shows higher CXCR7 and CXCL12 levels, underlining an inverse relation between receptors and ligands. Thus the sustained release of the respective chemokine, causing a constitutive paracrine/autocrine activation, might lead to receptor downregulation, analogously to what is observed in glioma stem cells.[48]

CXCR4 expression persists after in vivo PD-Mg-S engraftment in mouse embryos, although, when tumors develop, a significant expression of CXCR7 and E-cadherin (typical of PD-Mg-D) was also detected. Thus, stem cell differentiation may occur during in situ tumor formation to populate the growing mass. As observed in different CSCs,[46–49] both CXCL11 and CXCL12 trigger PD-Mg-S, but not PD-Mg-D, proliferation, chemotactic migration, and VM, acting as regulators of malignant behavior. This different responsiveness is independent from receptor mRNA expression, but resulting in the activation of different intracellular signals in the two cell populations (ERK1/2 activation and $[Ca^{2+}]i$ increase in PD-Mg-S vs. only ERK1/2 activation in PD-Mg-D), supporting a substantial functional difference among these cells. Thus, CXCL12 acts as full agonist in PD-Mg-S and biased-agonist in PD-Mg-D. When coexpressed, CXCR4 and CXCR7 can homo- or hetero-dimerize and the blockade of CXCL12-CXCR4/CXCR7 system was proposed as pharmacological approach in multiple tumors.[50] Pharmacological inhibition of CXCR4 or CXCR7 in PD-Mg-S abolished proliferation, migration, and VM induced by the respective ligands, indicating that these processes are mediated by both receptors. In CSCs isolated from several tumors, CXCR4 and CXCR7 act as heterodimers to determine the aggressive behavior of the neoplasia.[51,52] Although we did not provide a direct biochemical evidence, we show that the pharmacological inhibition of each receptor is sufficient to prevent CXCL12-mediated response, which is able to activate both CXCR4 and CXCR7. We hypothesize that in PD-Mg-S both antagonists may prevent ligand-induced CXCR4/CXCR7 dimer formation or block the signaling of preformed dimers (Figure 6C).

In conclusion, meningioma contains cell subpopulations endowed with CSC-like features, in which CXCL12/CXCL11/CXCR4/CXCR7 axis sustains the acquisition of an aggressive behavior (high cell proliferation, invasiveness, and neovascularization). Their characterization may help, altogether with the most advanced genetic classification, to provide a reliable prognostic assessment of meningioma in particular for those with apparent histological benign characteristics.

Overall, despite meningioma heterogeneity, CXCL11-12/CXCR4-7 network represents a general mechanism supporting meningioma stem-like cell functioning. Because chemokines are released by both tumor cells and TME, the role of CSCs should be considered when analyzing intra- and inter-tumor meningioma heterogeneity and the inhibition of this chemokine pathway may represent a possible strategy against aggressive/recurrent meningiomas.

Supplementary Material

Supplementary material is available online at *Neuro-Oncology* (http://neuro-oncology.oxfordjournals.org/).

Keywords

CXCL11/CXCL12 | meningioma | stem cells | tumorigenesis

Funding

V.F. and D.D.P.T. were supported by the grant AIRC-IG 2017 # 20106.

Acknowledgments

Authors thank M. Morini and IIT's Animal facility team for technical assistance on animal experiments.

Conflict of Interest

All authors have no conflict of interest to declare.

Authorship

designed research and experiments (FB, DDPT, and TF), performed experiments (AB, ID, AS, RW, VF, SR, DC, IA, GDL, MD, PS, MG, PM, NC, ST, AP, VF, and SR), collected, analyzed and interpreted data (FB, AB, VF, RW, PM, GZ, DDPT, and TF), drafted the manuscript (FB, DDPT, and TF); provided meningioma samples, and pathological and clinical patients' data (PN, PF, GG, and GZ); all authors read, revised, and approved the final version of the manuscript.

Data Availability

Dataset generated in this study are available through NCBI GEO dataset (GSE229670).

Affiliations

Section of Pharmacology, Department of Internal Medicine, University of Genova, Genova, Italy (FB., A.B., I.D., A.S., R.W., N.C., S.T., T.F.); IRCCS Ospedale Policlinico San Martino, Genova, Italy (D.C., G.D.L., M.D., P.N., P.F., G.G., P.M., A.P., G.Z., T.F.); Medical Physics Department, E.O. Galliera Hospital, Genova, Italy (P.S., M.G.); Department of Neurosciences, Rehabilitation, Ophthalmology, Genetics, Maternal and Child Health, University of Genova, Genova, Italy (G.Z., P.F.); Department of Experimental Medicine, University of Genova, Genova, Italy (I.A., P.M., A.P.); Neurobiology of miRNA, Istituto Italiano di Tecnologia (IIT), Genova, Italy (V.F., S.R., D.D.P.T.)

References

1. Ostrom QT, Patil N, Cioffi G, Waite K, Kruchko C, Barnholtz-Sloan JS. CBTRUS statistical report: Primary brain and other central nervous system tumors diagnosed in the United States in 2013-2017. *Neuro Oncol.* 2020;22(12 suppl 2):iv1–iv96.
2. Louis DN, Perry A, Reifenberger G, et al. The 2016 World Health Organization Classification of Tumors of the Central Nervous System: A summary. *Acta Neuropathol.* 2016;131(6):803–820.
3. Goldbrunner R, Stavrinou P, Jenkinson MD, et al. EANO guideline on the diagnosis and management of meningiomas. *Neuro Oncol.* 2021;23(11):1821–1834.
4. Nassiri F, Liu J, Patil V, et al. A clinically applicable integrative molecular classification of meningiomas. *Nature.* 2021;597(7874):119–125.
5. Gallagher MJ, Jenkinson MD, Brodbelt AR, Mills SJ, Chavredakis E. WHO grade 1 meningioma recurrence: Are location and Simpson grade still relevant? *Clin Neurol Neurosurg.* 2016;141:117–121.
6. Birzu C, Peyre M, Sahm F. Molecular alterations in meningioma: Prognostic and therapeutic perspectives. *Curr Opin Oncol.* 2020;32(6):613–622.
7. Florio T, Barbieri F. The status of the art of human malignant glioma management: The promising role of targeting tumor-initiating cells. *Drug Discov Today.* 2012;17(19–20):1103–1110.
8. Huang T, Song X, Xu D, et al. Stem cell programs in cancer initiation, progression, and therapy resistance. *Theranostics.* 2020;10(19):8721–8743.
9. Rath P, Miller DC, Litofsky NS, et al. Isolation and characterization of a population of stem-like progenitor cells from an atypical meningioma. *Exp Mol Pathol.* 2011;90(2):179–188.
10. Tang H, Zhu H, Wang X, et al. KLF4 is a tumor suppressor in anaplastic meningioma stem-like cells and human meningiomas. *J Mol Cell Biol.* 2017;9(4):315–324.
11. Freitag D, McLean AL, Simon M, et al. NANOG overexpression and its correlation with stem cell and differentiation markers in meningiomas of different WHO grades. *Mol Carcinog.* 2017;56(8):1953–1964.
12. Lim HY, Kim KM, Kim BK, et al. Isolation of mesenchymal stem-like cells in meningioma specimens. *Int J Oncol.* 2013;43(4):1260–1268.
13. Hu D, Wang X, Mao Y, Zhou L. Identification of CD105 (endoglin)-positive stem-like cells in rhabdoid meningioma. *J Neurooncol.* 2012;106(3):505–517.
14. Kannapadi NV, Shah PP, Mathios D, Jackson CM. Synthesizing molecular and immune characteristics to move beyond WHO grade in meningiomas: A focused review. *Front Oncol.* 2022;12:892004.
15. Lopez-Gil JC, Martin-Hijano L, Hermann PC, Sainz B, Jr. The CXCL12 crossroads in cancer stem cells and their niche. *Cancers.* 2021;13(3):469.
16. Gao Q, Zhang Y. CXCL11 signaling in the tumor microenvironment. *Adv Exp Med Biol.* 2021;1302:41–50.
17. Shi Y, Riese DJ, 2nd, Shen J. The role of the CXCL12/CXCR4/CXCR7 chemokine axis in cancer. *Front Pharmacol.* 2020;11:574667.
18. Luker KE, Gupta M, Luker GD. Imaging chemokine receptor dimerization with firefly luciferase complementation. *FASEB J.* 2009;23(3):823–834.
19. Bajetto A, Barbieri F, Pattarozzi A, et al. CXCR4 and SDF1 expression in human meningiomas: A proliferative role in tumoral meningothelial cells in vitro. *Neuro Oncol.* 2007;9(1):3–11.
20. Barbieri F, Bajetto A, Porcile C, et al. CXC receptor and chemokine expression in human meningioma: SDF1/CXCR4 signaling activates ERK1/2 and stimulates meningioma cell proliferation. *Ann N Y Acad Sci.* 2006;1090(1):332–343.
21. Wurth R, Barbieri F, Bajetto A, et al. Expression of CXCR7 chemokine receptor in human meningioma cells and in intratumoral microvasculature. *J Neuroimmunol.* 2011;234(1–2):115–123.
22. Hoffmann N, Fernandez V, Pereira RC, et al. A xenotransplant model of human brain tumors in wild-type mice. *iScience.* 2020;23(1):100813.
23. Arena S, Barbieri F, Thellung S, et al. Expression of somatostatin receptor mRNA in human meningiomas and their implication in in vitro antiproliferative activity. *J Neurooncol.* 2004;66(1–2):155–166.
24. Bajetto A, Porcile C, Pattarozzi A, et al. Differential role of EGF and BFGF in human GBM-TIC proliferation: Relationship to EGFR-tyrosine kinase inhibitor sensibility. *J Biol Regul Homeost Agents.* 2013;27(1):143–154.
25. Dominici M, Le Blanc K, Mueller I, et al. Minimal criteria for defining multipotent mesenchymal stromal cells. The International Society for Cellular Therapy position statement. *Cytotherapy.* 2006;8(4):315–317.
26. Li F, Xu J, Liu S. Cancer stem cells and neovascularization. *Cells.* 2021;10(5):1070.
27. De Clercq E. The bicyclam AMD3100 story. *Nat Rev Drug Discov.* 2003;2(7):581–587.
28. Zabel BA, Wang Y, Lewen S, et al. Elucidation of CXCR7-mediated signaling events and inhibition of CXCR4-mediated tumor cell transendothelial migration by CXCR7 ligands. *J Immunol.* 2009;183(5):3204–3211.
29. Barbieri F, Bosio AG, Pattarozzi A, et al. Chloride intracellular channel 1 activity is not required for glioblastoma development but its inhibition dictates glioma stem cell responsivity to novel biguanide derivatives. *J Exp Clin Cancer Res.* 2022;41(1):53.
30. Hubert CG, Rivera M, Spangler LC, et al. A three-dimensional organoid culture system derived from human glioblastomas recapitulates the

hypoxic gradients and cancer stem cell heterogeneity of tumors found in vivo. *Cancer Res.* 2016;76(8):2465–2477.

31. Bayley JC, Hadley CC, Harmanci AO, et al. Multiple approaches converge on three biological subtypes of meningioma and extract new insights from published studies. *Sci Adv.* 2022;8(5):eabm6247.
32. Wurth R, Barbieri F, Pattarozzi A, et al. Phenotypical and pharmacological characterization of stem-like cells in human pituitary adenomas. *Mol Neurobiol.* 2017;54(7):4879–4895.
33. Kilmister EJ, Patel J, Bockett N, et al. Embryonic stem cell-like subpopulations are present within Schwannoma. *J Clin Neurosci.* 2020;81:201–209.
34. Shivapathasundram G, Wickremesekera AC, Brasch HD, et al. Expression of embryonic stem cell markers on the microvessels of WHO grade i meningioma. *Front Surg.* 2018;5:65.
35. Nigim F, Esaki S, Hood M, et al. A new patient-derived orthotopic malignant meningioma model treated with oncolytic herpes simplex virus. *Neuro Oncol.* 2016;18(9):1278–1287.
36. Hueng DY, Sytwu HK, Huang SM, Chang C, Ma HI. Isolation and characterization of tumor stem-like cells from human meningiomas. *J Neurooncol.* 2011;104(1):45–53.
37. Maier AD, Mirian C, Bartek J, Jr, et al. Expression of the stem cell marker CD133 in malignant meningioma. *Clin Neuropathol.* 2021;40(3):151–159.
38. Kamamoto D, Saga I, Ohara K, Yoshida K, Sasaki H. Association between CD133, CD44, and nestin expression and prognostic factors in high-grade meningioma. *World Neurosurg.* 2018;124:e188–e196.
39. Alamir H, Alomari M, Salwati AAA, et al. In situ characterization of stem cells-like biomarkers in meningiomas. *Cancer Cell Int.* 2018;18:77.
40. He JH, Wang J, Yang YZ, et al. SSTR2 is a prognostic factor and a promising therapeutic target in glioma. *Am J Transl Res.* 2021;13(10):11223–11234.
41. Boetto J, Peyre M, Kalamarides M. Meningiomas from a developmental perspective: Exploring the crossroads between meningeal embryology and tumorigenesis. *Acta Neurochir (Wien).* 2021;163(1):57–66.
42. Wallesch M, Pachow D, Blucher C, et al. Altered expression of E-Cadherin-related transcription factors indicates partial epithelial-mesenchymal transition in aggressive meningiomas. *J Neurol Sci.* 2017;380:112–121.
43. Utsuki S, Oka H, Sato Y, et al. Invasive meningioma is associated with a low expression of E-cadherin and beta-catenin. *Clin Neuropathol.* 2005;24(1):8–12.
44. Kirches E, Steffen T, Waldt N, et al. The expression of the MSC-marker CD73 and of NF2/Merlin are correlated in meningiomas. *J Neurooncol.* 2018;138(2):251–259.
45. Kliese N, Gobrecht P, Pachow D, et al. miRNA-145 is downregulated in atypical and anaplastic meningiomas and negatively regulates motility and proliferation of meningioma cells. *Oncogene.* 2013;32(39):4712–4720.
46. Barbieri F, Bajetto A, Stumm R, et al. Overexpression of stromal cell-derived factor 1 and its receptor CXCR4 induces autocrine/paracrine cell proliferation in human pituitary adenomas. *Clin Cancer Res.* 2008;14(16):5022–5032.
47. Wurth R, Bajetto A, Harrison JK, Barbieri F, Florio T. CXCL12 modulation of CXCR4 and CXCR7 activity in human glioblastoma stem-like cells and regulation of the tumor microenvironment. *Front Cell Neurosci.* 2014;8:144.
48. Gatti M, Pattarozzi A, Bajetto A, et al. Inhibition of CXCL12/CXCR4 autocrine/paracrine loop reduces viability of human glioblastoma stem-like cells affecting self-renewal activity. *Toxicology.* 2013;314(2–3):209–220.
49. Uemae Y, Ishikawa E, Osuka S, et al. CXCL12 secreted from glioma stem cells regulates their proliferation. *J Neurooncol.* 2014;117(1):43–51.
50. Huynh C, Dingemanse J, Meyer Zu Schwabedissen HE, Sidharta PN. Relevance of the CXCR4/CXCR7-CXCL12 axis and its effect in pathophysiological conditions. *Pharmacol Res.* 2020;161:105092.
51. Del Molino Del Barrio I, Wilkins GC, Meeson A, Ali S, Kirby JA. Breast cancer: An examination of the potential of ACKR3 to modify the response of CXCR4 to CXCL12. *Int J Mol Sci.* 2018; 19(11):3592.
52. Song ZY, Wang F, Cui SX, Gao ZH, Qu XJ. CXCR7/CXCR4 heterodimer-induced histone demethylation: A new mechanism of colorectal tumorigenesis. *Oncogene.* 2019;38(9):1560–1575.